J. Cent. South Univ. (2015) 22: 2578−2585
DOI: 10.1007/s11771-015-2787-0

Springer

Thermal-hydraulic modeling and analysis of hydraulic system by pseudo-bond graph

HU Jun-ping(胡均平), LI Ke-jun(李科军)

College of Mechanical and Electrical Engineering, Central South University, Changsha 410083, China

Abstract: To increase the efficiency and reliability of the thermodynamics analysis of the hydraulic system, the method based on pseudo-bond graph is introduced. According to the working mechanism of hydraulic components, they can be separated into two categories: capacitive components and resistive components. Then, the thermal-hydraulic pseudo-bond graphs of capacitive C element and resistance R element were developed, based on the conservation of mass and energy. Subsequently, the connection rule for the pseudo-bond graph elements and the method to construct the complete thermal-hydraulic system model were proposed. On the basis of heat transfer analysis of a typical hydraulic circuit containing a piston pump, the lumped parameter mathematical model of the system was given. The good agreement between the simulation results and experimental data demonstrates the validity of the modeling method.

Key words: thermodynamics; hydraulic system; pseudo-bond graph; piston pump; modeling; temperature simulation

1 Introduction

The temperature change of oil in hydraulic system has an important influence on the working performance of the system. If the temperature of oil is too high or too low, it will result in a negative effect on the normal operation of the system and even make the system not work properly [1−2]. Specially, for some precision hydraulic equipment, the fluctuation of the oil temperature will seriously affect the control precision of the system. Therefore, with the increase in hydraulic system power densities and higher control accuracy, it is necessary to construct the thermal-hydraulic model of some hydraulic systems to predict the system pressure and temperature response.

Many studies on thermal-hydraulic analysis for the hydraulic system have been reported. SIDDERS et al [3] derived the basic formulas for modeling the thermal hydraulic components. ZHANG et al [4] proposed the thermal-hydraulic model of landing gear retraction system, and demonstrated the effects of oil temperature change on the system performance. To reduce the simulation time, LI and JIAO [5] researched the calculation method for thermal-hydraulic system simulation, which was applied to the position-controlled thermal-hydraulic system. HAN et al [6] developed the thermodynamics model of the piston pump with consideration of all kinds of heat transfer. WANG et al [7] rearranged the oil cooler in the returned circuit to ensure that the components operate and are maintained within pre-defined oil temperature. LIANG et al [8] presented a thermodynamic model of a shock absorber, and the evolution of the temperatures of the absorber was obtained by solving the equations derived from the model, which was verified experimentally. However, these studies failed to efficiently establish the thermal-hydraulic model of the hydraulic system in a unified way, specially, when the thermodynamic behavior of hydraulic system is coupled with dynamic behavior of mechanical system or other energy domain system. The traditional modeling method [3−9] was usually focused on the single domain system, and the equations of multi-energy domains must be connected by the intermediate variables, so the system modeling becomes complex and errors occur. To improve this situation, other analytical approach such as bond graph method based on energy and information flow is considered to be more desirable in the present work. This allows to study the structure of the system model. The nature of the parts of the model and the manner in which the parts interact can be made evidently in a graphical format. The system equations can also be derived algorithmically in a systematic manner when the overall

Foundation item: Project(51175518) supported by the National Natural Science Foundation of China
Received date: 2014−06−24; **Accepted date:** 2014−11−08
Corresponding author: LI Ke-jun, PhD Candidate; Tel: +86−13548948786; E-mali: likejuncsu@126.com

bond graph is ready [10−12]. KARNOPP et al [11] proposed the concept of pseudo-bond graph for the thermo-fluid systems, the temperature and pressure are defined as effort variables, and the corresponding flow variables are energy flow and mass flow. Apart from the restriction that the product of the variables associated with each bond does not equal the instantaneous power, pseudo-bond graphs share all other features with true bond graphs. But it is only applied to the study of compressible gas, and the thermo-hydraulic system needs to be further researched.

In the present work, according to the experience of pseudo-bond graph applied to the pneumatic system [13], the thermal-hydraulic pseudo-bond graph of capacitive (C) and resistance (R) elements are developed based on the conservation of mass and energy, and the connection rule for the two elements was also studied. Subsequently, the method to generate the complete thermal-hydraulic system model based on the pseudo-bond graph is proposed, which is used to establish the lumped parameter mathematical model of a typical hydraulic circuit containing a piston pump.

2 Pseudo-bond graph elements for thermal-hydraulic model

There is a wide variety of hydraulic components due to their function, working principle, structure, etc. However, considering the working mechanism of the hydraulic components [14], they can be separated into two categories: the capacitive components (C) and the resistance (R) components.

2.1 Pseudo-bond graph C element for capacitive components

The hydraulic pipeline, the cylinder chamber, the accumulator, etc, are the basic capacitive components in hydraulic system. The basic capacitive components can be regarded as the control volume in which the pressure and the temperature can be computed. The conservation equations of mass and energy are the basic equations for thermal-hydraulic modeling of the capacitive components. As shown in Fig. 1, the changing rate of mass flow in the control volume can be described as

$$\dot{m} = \sum \dot{m}_{\rm i} - \sum \dot{m}_{\rm o} \tag{1}$$

where $\dot{m}_{\rm i}$ is the flow rate of mass into the control volume, and $\dot{m}_{\rm o}$ is the flow rate of mass out of the control volume.

At any time, the mean fluid density in the control volume is given by

$$\rho = m / V \tag{2}$$

Combined with Eq. (1), the time derivative of ρ can be expressed as

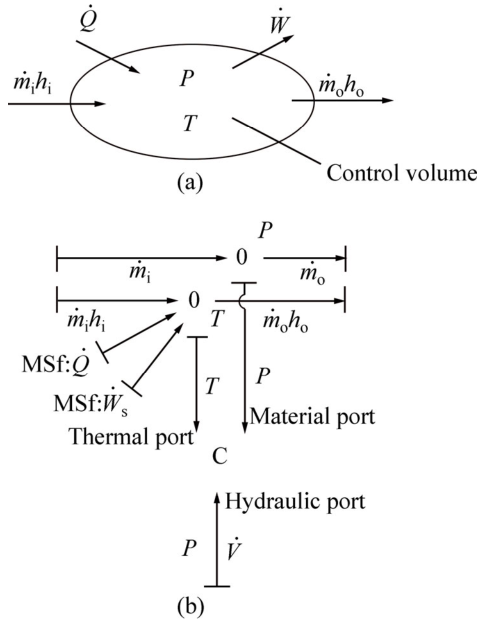

Fig. 1 Control volume (a) and pseudo-bond graph C element (b)

$$\dot{\rho} = \frac{\dot{m} - \rho \dot{V}}{V} \tag{3}$$

where V is the volume of the control volume.

Considering the thermodynamic properties of the fluid, the density can be expressed as a function of pressure and temperature:

$$\rho = \rho(P,\ T) \tag{4}$$

By differentiating with respect to temperature and pressure, Eq. (4) leads to

$$\mathrm{d}\rho = \left(\frac{\partial \rho}{\partial P}\right)_T \mathrm{d}P + \left(\frac{\partial \rho}{\partial T}\right)_P \mathrm{d}T \tag{5}$$

From Eq. (5), pressure in the control volume can be computed by

$$\mathrm{d}P = \frac{1}{\left(\dfrac{\partial \rho}{\partial P}\right)_T}\left[\mathrm{d}\rho - \left(\frac{\partial \rho}{\partial T}\right)_P \mathrm{d}T\right] \tag{6}$$

The isothermal bulk modulus β_T and the cubical expansion coefficient α_P are defined as follow:

$$\begin{cases} \beta_T = \rho(\dfrac{\partial P}{\partial \rho})_T \\ \alpha_P = -\dfrac{1}{\rho}(\dfrac{\partial \rho}{\partial T})_P \end{cases} \tag{7}$$

Substituting Eq.（7）into Eq.（6）and differentiating with respect to time lead to

$$\dot{P} = \beta_T \left[\frac{1}{\rho}\dot{\rho} + \alpha_P \dot{T}\right] \tag{8}$$

Combining Eq. (1), Eq. (3) and Eq. (8) gives

$$\dot{P} = \beta_T \left[\frac{1}{\rho V} \left(\sum \dot{m}_i - \sum \dot{m}_o - \rho \dot{V} \right) + \alpha_P \dot{T} \right] \tag{9}$$

For one-dimensional flow, the energy conservation equation for the control volume can be written as

$$\dot{Q} - \dot{W} = \sum \dot{m}_o h_o - \sum \dot{m}_i h_i + \dot{E} \tag{10}$$

where $\dot{Q}$ represents heat flow absorbed by the control volume from outside, including heat transfer and heat radiation. $\dot{W}$ is the rate of work except for the work required to push mass into and out of the control volume. $\dot{E}$ is the time rate of change of the fluid energy in the control volume. h_i is the specific enthalpy of the fluid flowing into the control volume. h_o is the specific enthalpy of the fluid flowing out of the control volume.

Energy in the control volume can also be expressed as

$$E = u + E_K + E_P \tag{11}$$

where u is the internal energy, E_K is the kinetic energy and E_P is the potential energy. Generally, E_K and E_P are very small compared with u, so they can be ignored. As a result, the time rate of change of the fluid energy in the control volume can rewritten as

$$\dot{E} = m\dot{u} + u\dot{m} \tag{12}$$

It is assumed that the phase of fluid in the control volume does not change, so the fluid enthalpy can be defined as

$$h = u + Pv \tag{13}$$

where h is the fluid enthalpy, P is the fluid pressure, and v is the specific volume.

The time rate of change of the fluid enthalpy is calculated as follows [15−16]:

$$\dot{h} = C_P \dot{T} + (1 - \alpha_P T) v \dot{P} \tag{14}$$

where $\dot{T}$ is the temperature of the fluid in the control volume, α_P is the fluid volume expansion coefficient, and C_P is the specific heat of the fluid.

After introducing Eq. (14) and Eq. (13) into Eq. (12), Eq. (15) is obtained:

$$\dot{E} = C_P m \dot{T} - mT\alpha_P v \dot{P} + h\dot{m} - P\dot{V} \tag{15}$$

Combining Eq. (1), Eq. (10) and Eq. (15) gives

$$\dot{T} = \frac{1}{C_P m} \left[\sum \dot{m}_i (h_i - h) + \sum \dot{m}_o (h - h_o) + \dot{Q} - \dot{W} + P\dot{V} + \frac{mT\alpha_P}{\rho} \dot{P} \right] \tag{16}$$

where $\dot{W}$ represents the rate of boundary work and shaft work. It can be written as

$$\dot{W} = \dot{W}_s + \dot{W}_b = \dot{W}_s + P\dot{V} \tag{17}$$

Introducing Eq. (16) into Eq. (15) gives

$$\dot{T} = \frac{1}{C_P m} \left[\sum \dot{m}_i (h_i - h) + \sum \dot{m}_o (h - h_o) + \dot{Q} - \dot{W}_s + \frac{mT\alpha_P}{\rho} \dot{P} \right] \tag{18}$$

Generally, it is assumed that the average enthalpy within the control volume is equal to the leaving enthalpy regardless of the inlet conditions [5]. Equation (18) can be rewritten as

$$\dot{T} = \frac{1}{C_P m} \left[\sum \dot{m}_i (h_i - h) + \dot{Q} - \dot{W}_s + T\alpha_P V \dot{P} \right] \tag{19}$$

Equations (9) and (19) are the lumped parameter equations representing conservation of mass and energy, respectively.

Obviously, the two equations are cross coupled. Therefore, fast pressure transients will produce fast temperature transients and vice versa [5]. Meanwhile, according to the two equations, state variables $\dot{P}$ and $\dot{T}$ are defined as effort variables of the pseudo-bond graph C element, and state variables $\dot{m}$, $\dot{V}$, $\dot{Q}$ and $\dot{W}_s$ can be defined as flow variables of the pseudo-bond graph C element (as show in Fig. 1). The C element has three ports, namely, thermal port, material port and hydraulic port. Summation of flows at the 0-junction connected to the thermal port of the C element yields the energy balance of Eq. (19), and the second 0-junction connected to the material port represents the mass balance of Eq. (9). The thermodynamic accumulator can be linked with a bond graph of a mechanical subsystem via a transformer [17].

2.2 Pseudo-bond graph R element for resistance components

As shown in Fig. 2, the throttle valve, directional valve, oil filter, etc, are typical resistance components. The mass flow rate through the resistive components depends on the concrete resistive structure and the fluid state. For example, the standard orifice turbulent mass flow equation is given by [18]

$$\dot{m} = \rho \dot{V} = \rho c_d A \sqrt{2\rho (P_1 - P_2)} \tag{20}$$

It is assumed that the fluid enthalpy of the flow

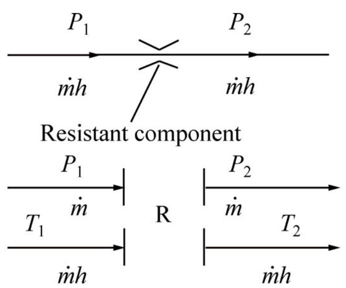

Fig. 2 Pseudo-bond graph R element

through the resistive component does not change, so the power consumption converting into heat can be computed by

$$\dot{Q}_{\mathrm{r}} = \Delta p \dot{Q} = c_{\mathrm{d}} A \sqrt{2(P_1 - P_2)^3 / \rho} \tag{21}$$

According to the above two equations, state variables $\dot{P}$ and $\dot{T}$ are defined as effort variables of the pseudo-bond graph R element, and the state variables $\dot{m}$, $\dot{V}$, $\dot{Q}$ and $\dot{W}_{\mathrm{s}}$ can be defined as flow variables of the pseudo-bond graph R element. It is apparent that the input variables of resistive component are pressure and temperature, which are just the output variables of capacitive component. The output variables of resistive component are mass flow rate and heat flow rate, which can be used in the capacitive component, so the connection rule for the two pseudo-bond graph elements can be determined, as shown in Fig. 3.

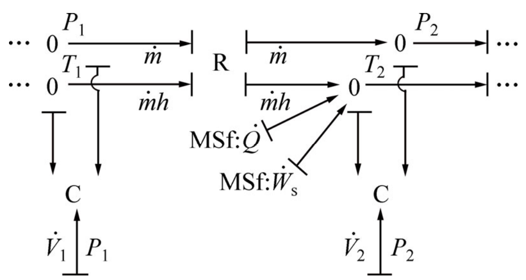

Fig. 3 Connection rule for two pseudo-bond graph elements

2.3 Heat transfer calculation

In the hydraulic system, the control volume is a closed space surrounded by metal shell or hydraulic pipelines. If the temperature difference exists between the fluid in the control volume and the shell, the heat transfer will occur inevitably by convection. The heat exchange between the control volume and the shell is given by

$$\dot{Q}_{\mathrm{t}} = KA(T_{\mathrm{f}} - T_{\mathrm{w}}) \tag{22}$$

where K is the fluid/shell heat transfer coefficient, A is the heat transfer area inside the shell, T_{f} is the fluid temperature, and T_{w} is the shell temperature. In Eq. (21) and Eq. (22), it can be seen that the heat transferred to the control volume consists of two parts: one part is generated by the resistant components, and the other is transferred from the body shell.

For the wall/ambient interface, the heat transferred by radiation is calculated by

$$\dot{Q}_{\mathrm{rad}} = \varepsilon \sigma A_{\mathrm{r}} (T_{\mathrm{h}}^4 - T_{\mathrm{w}}^4) \tag{23}$$

where ε is emissivity of the shell, σ is the Stefan-Boltzmann constant, A_{r} is the area of the radiation, and T_{h} is the ambient temperature.

3 Circuit description

Figure 4 shows a thermal-hydraulic model of a typical hydraulic circuit, which consists of a piston pump, adjustable throttle valve and reservoir. The control volume o represents the volume between the valve plate and throttle valve. The control volume e indicates the volume between the rotating part and the shell of the pump. The control volume i represents the volume of oil in the tank. T_{o}, T_{e} and T_{i} are the temperatures of oil in the three control volumes, respectively. As for the pump, T_{r} and T_{s} are the temperatures of the rotating part and the shell part of pump, respectively. The oil is supplied into the inlet port of the pump with the temperature T_{i}, which is under the action of plunger to flow across the valve plate and into the control volume o. In this process, there will be fluid power loss P_{d} and viscous friction power loss P_{n}, and the heat generated by the power loss also transfers to the control volume o. The heat $\dot{Q}_{\mathrm{l}}$ converted from leakage resistance of pump transfers to the control

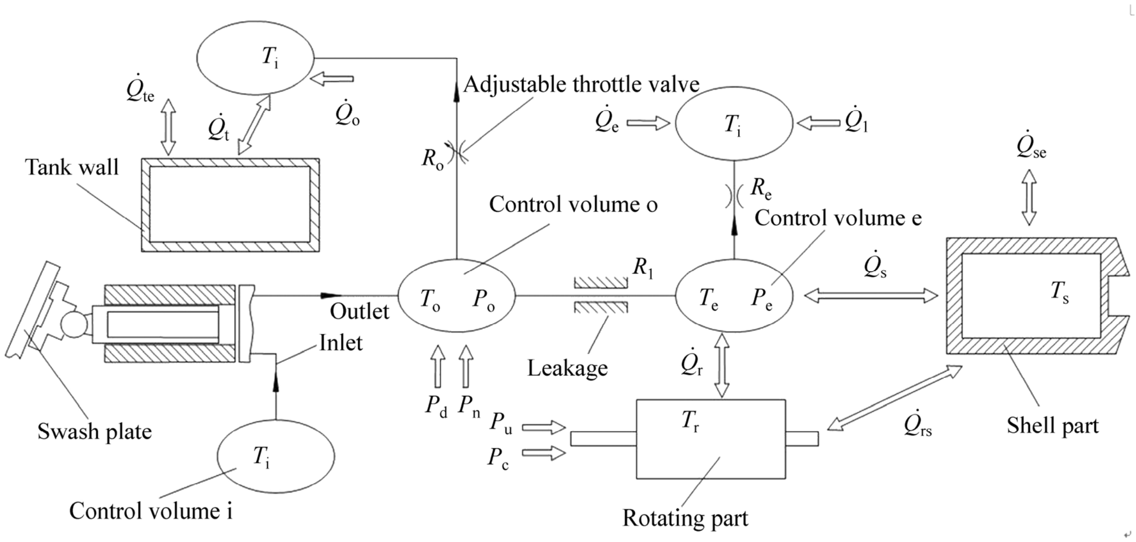

Fig. 4 A typical hydraulic circuit for thermal analysis

volume e. $\dot{Q}_r$ represents the heat exchange between the oil in the control volume e and the rotating part of pump. $\dot{Q}_s$ represents the heat exchange between the oil in the control volume e and the shell part of pump. The heat $\dot{Q}_e$ generated by the resistance of return pipe transfers to the control volume i. P_u and P_c represent the dry friction loss of the pump and constant friction loss, which can be assumed to transfer directly to the rotating part of the pump. $\dot{Q}_{rs}$ represents the heat transfer between the shell part and the rotation part of the pump. Meanwhile, there is heat transferred by radiation and convection between the shell part and the ambient, which is calculated by $\dot{Q}_{se}$. The power consumption of the throttle valve can be described by the standard orifice turbulent flow equation, which converts to heat and transfers to the control volume i. $\dot{Q}_t$ represents the heat exchanged between the oil in the tank and the tank wall. $\dot{Q}_{te}$ represents the heat transferred by radiation and convection between the tank wall and the ambient.

4 Mathematical models

In the development of the thermal-hydraulic model of the typical hydraulic system, the following assumptions are made:

1) The pressure and temperature of the control volume are assumed to be uniform at any given instant, and the mixture is ideal.

2) The capacitive and resistive effects are lumped whenever appropriate.

3) The speed of the pump is constant, and the fluctuation of the flow is neglected.

4) The leakage flow of the pump is considered to be laminar.

5) The fluid inertia is neglected.

According to the direction of generalized power flow, the complete bond graph model of the hydraulic system is made, as shown in Fig. 5.

It can be found that the model mainly consists of six parts: the control volume e, the control volume o, the control volume i, the tank wall, the rotation part and shell part of the pump. The pseudo-bond graph elements C_e, C_o and C_i represent the capacitive effect of the control volumes, in which the pressure and temperature can be computed accordingly. The temperatures of the tank wall, the rotation part and shell part of the pump are T_t, T_r and T_s, respectively. c_t, c_r and c_s elements are the corresponding thermal capacities. R_t, R_r and R_s elements represent the corresponding thermal resistances. R_l element represents the leakage resistance of the pump, through which the mass flow $\dot{m}_l$ passes into tank. R_o element represents the resistance of throttle valve, through which the mass flow $\dot{m}_o$ depends on the port opening area. The hydraulic resistance of return pipeline is taken into account by R_e element, through which the mass flow $\dot{m}_e$ returns to tank. The constant effort source Se:T_a element represents the temperature of the ambient. The flow sources Sf:Q_d and Sf:Q_n elements represent the heat generated by the fluid power loss P_d and viscous friction loss P_n. The flow sources Sf:Q_o and Sf:Q_e elements represent the thermal power due to throttling loss and leakage loss.

The time derivative of the pressure and temperature of fluid in the control volume o can be described as

$$\dot{P}_o = \beta_T \left[\frac{1}{\rho V_o} \left(\dot{m}_i - \dot{m}_o - \dot{m}_l \right) + \alpha_P \dot{T}_o \right] \tag{24}$$

$$\dot{T}_o = \frac{1}{C_P m_o} \left[\sum \dot{m}_i (h_i - h_o) + \dot{Q}_n + \dot{Q}_d + T_o \alpha_P V_o \dot{P}_o \right] \tag{25}$$

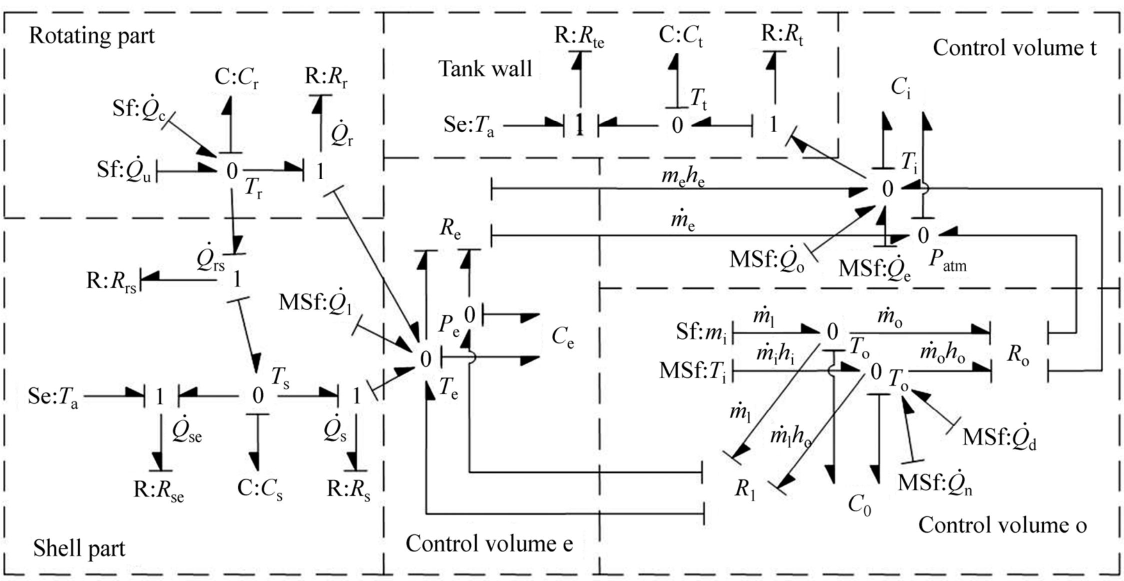

Fig. 5 Bond graph model of pump

The time derivative of the pressure and temperature of fluid in the control volume e can be calculated by

$$\dot{P}_{\mathrm{e}} = \beta_T \left[\frac{1}{\rho V_{\mathrm{e}}} \left(\dot{m}_{\mathrm{l}} - \dot{m}_{\mathrm{e}} \right) + \alpha_P \dot{T}_{\mathrm{e}} \right] \tag{26}$$

$$\dot{T}_{\mathrm{e}} = \frac{1}{C_P m_{\mathrm{e}}} \left[\sum \dot{m}_{\mathrm{l}} (h_{\mathrm{o}} - h_{\mathrm{e}}) + \dot{Q}_{\mathrm{l}} + T_{\mathrm{e}} \alpha_P V_{\mathrm{e}} \dot{P}_{\mathrm{e}} \right] \tag{27}$$

The time derivative of the temperature in control volume i can be written as

$$\dot{T}_{\mathrm{i}} = \frac{1}{C_P m_{\mathrm{i}}} \left[m_{\mathrm{o}} (h_{\mathrm{o}} - h_{\mathrm{i}}) + m_{\mathrm{e}} (h_{\mathrm{e}} - h_{\mathrm{i}}) + \dot{Q}_{\mathrm{o}} + \dot{Q}_{\mathrm{e}} - \frac{T_{\mathrm{i}} - T_{\mathrm{t}}}{R_{\mathrm{t}}} \right] \tag{28}$$

The time derivative of the temperature of tank wall can be written as

$$\dot{T}_{\mathrm{t}} = \frac{1}{C_{\mathrm{t}} m_{\mathrm{t}}} \left[\frac{T_{\mathrm{i}} - T_{\mathrm{t}}}{R_{\mathrm{t}}} - \frac{T_{\mathrm{t}} - T_{\mathrm{a}}}{R_{\mathrm{ta}}} \right] \tag{29}$$

The time derivative of the temperature at the rotation part of pump can be written as

$$\dot{T}_{\mathrm{r}} = \frac{1}{C_{\mathrm{r}} m_{\mathrm{r}}} \left[\dot{Q}_{\mathrm{c}} + \dot{Q}_{\mathrm{u}} - \frac{T_{\mathrm{r}} - T_{\mathrm{e}}}{R_{\mathrm{r}}} - \frac{T_{\mathrm{r}} - T_{\mathrm{s}}}{R_{\mathrm{rs}}} \right] \tag{30}$$

The time derivative of the temperature at the shell part of pump can be written as

$$\dot{T}_{\mathrm{s}} = \frac{1}{C_{\mathrm{s}} m_{\mathrm{s}}} \left[\frac{T_{\mathrm{r}} - T_{\mathrm{s}}}{R_{\mathrm{rs}}} - \dot{Q}_{\mathrm{s}} - \dot{Q}_{\mathrm{sa}} \right] \tag{31}$$

The calculation of the heat transfer in the above equations can be referred to Refs. [19−21].

5 Simulation results

The simulated system is shown in Fig. 6. To validate the correctness of this modeling method, the pressure sensor is installed at the outlet port of the pump, and the temperature sensors are installed at the inlet port, outlet port and leakage port of the pump. In the initial state of the system, the pressure of the outlet port of the pump is set at 8 MPa by adjusting the throttle valve. In this work, the total experiment time is 30 min. The main parameters used in the simulation are listed in Table 1.

The comparison of the simulated and experimental pressure and temperature are shown in Fig. 7 and Fig. 8.

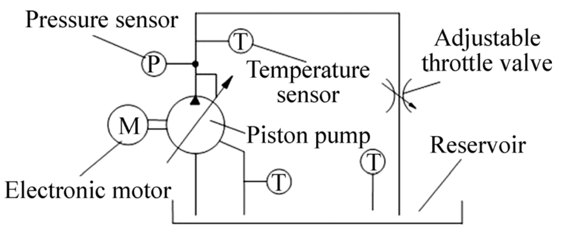

Fig. 6 Test rig for thermal-hydraulic analysis of piston pump

Table 1 Main parameters for thermodynamic calculation and simulation

Parameter	Value
Leakage coefficient of pump	1×10^{-9}
Displacement of pump/(mL·r^{-1})	10
Radiating area of pump/m^2	0.35
Radiating area of tank/m^2	4.33
Mass of rotation part of pump/kg	12
Mass of shell part of pump/kg	17
Emissivity of shell	0.32
Ambient temperature/°C	20
Speed of motor/(r·min^{-1})	1450

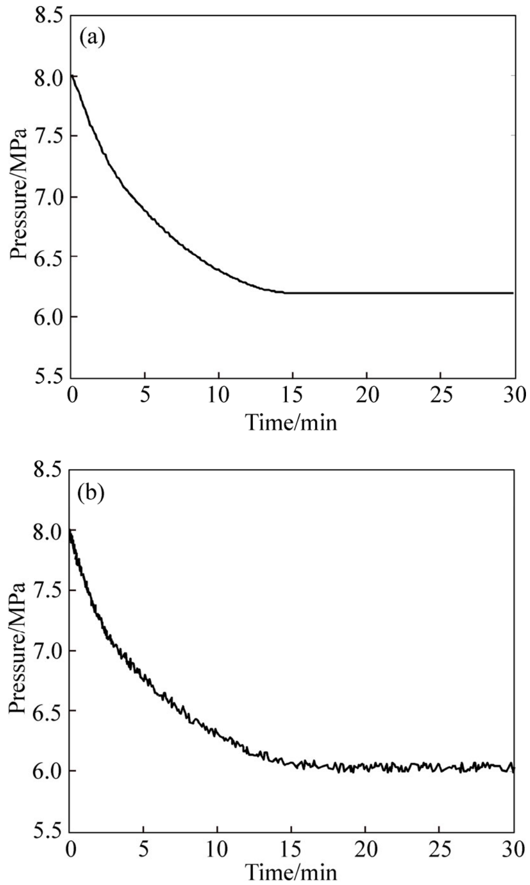

Fig. 7 Comparison between simulated (a) and experimental (b) results of pressure at outlet port of pump

The following conclusions can be made.

1) The experimental results show that the response is of higher order form with the significant ripples in the transient values. This is mainly due to the couple of the output flow pulsation of the pump and the vibration of the pipeline. While in simulation, the output flow of the pump is assumed to be a constant value, and the vibration of the pipeline is also omitted.

2) In experiment, the rate of pressure decline at outlet port of the pump and the rate of temperature rise at all ports of the pump are greater than those of simulation

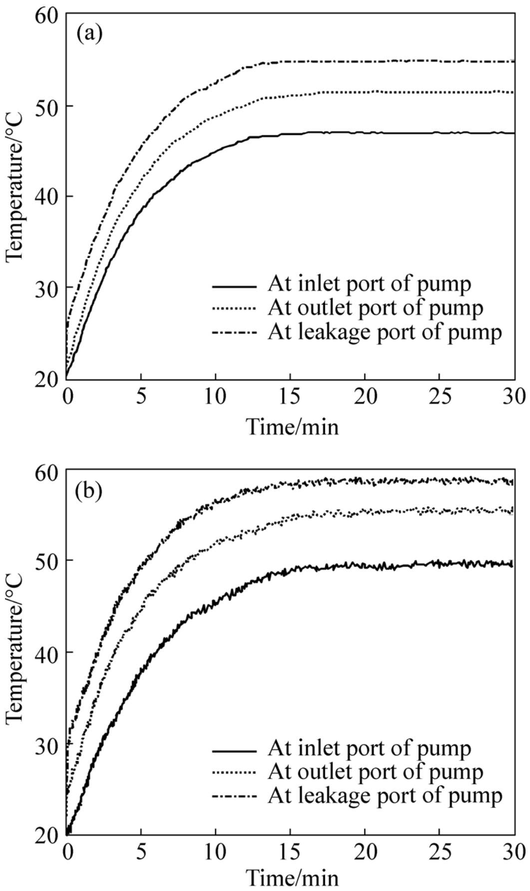

Fig. 8 Comparison between simulation (a) and experimental (b) results of temperature at all ports of pump

results. At last, the system is steady at about 17.5 min, which is increased by about 4.5 min compared with the simulation result.

3) The steady state pressure at the outlet port of the pump and the steady state temperatures at the inlet port, outlet port and leakage port of the pump are 6.2 MPa, 49.3 °C, 56.2 °C and 58.5 °C, respectively; while in simulation, they are 6 MPa, 46.9 °C, 51.5 °C and 55 °C, respectively. It is apparent that there are about 10% errors between the simulation results and experimental data that may be attributed to the differences between the calculated and actual values of the system parameters.

From the above analysis, the agreement between the simulation data and experimental results is acceptable for the application in this work, which indicates that this modeling method can be used to analyze and predict the temperature and pressure responses of the hydraulic system.

6 Conclusions

1) According to the working mechanism of hydraulic components, they can be separated into two categories: capacitive components and resistive components. Then, the thermal-hydraulic pseudo-bond graph C and R elements for the capacitive components and resistive components are proposed. Subsequently, the connection rule for basic thermal-hydraulic pseudo-bond graph elements and the method to automatically generate the complete thermal-hydraulic system model are put forward, which are applied to the model of a typical hydraulic system. The simulation and experiment are carried out to verify this modeling method. The good agreement between the simulation results and experimental data shows that this modeling method can be applied to any hydraulic system to predict the transient and steady state response.

2) The pseudo-bond graph C and R elements are basic components for the thermodynamic analysis of hydraulic system. The hydraulic components in the hydraulic circuit can be abstracted as capacitive elements and resistant elements, and then, the complete bond graph model of hydraulic system can be developed quickly by the connection rule mentioned above. This modeling method provides a new research idea for the temperature simulation of hydraulic system and expands the simulation range of the bond graph theory. In addition, by using hydraulic port of pseudo-bond graph C element, it is easy to combine with the subsystems of electromechanical part to construct a globally coupled dynamic model of the system.

References

[1] LI Yong-lin, XU Hao-jun, CAO Liang-mou. Efficiency analysis and thermal-hydraulic modeling of aerial piston pump at whole work condition [J]. Journal of Beijing University of Aeronautics and Astronautics, 2010, 36(12): 1469−1472. (in Chinese)

[2] LIU Wen-ping, WANG Lin-tao, JIANG Zhao-liang. Oil temperature analysis and determination of slippage pump discharge of closed hydraulic system [J]. Journal of Central South University (Science and Technology), 2013, 44(9): 3658−3664. (in Chinese)

[3] SIDDERS J A, TILLEY D G, CHAPPIE P J. Thermal-hydraulic performance prediction in fluid power systems [J]. Proceedings of the Institution of Mechanical Engineers, Part I: Journal of Systems and Control Engineering, 1996, 210(4): 231−242.

[4] ZHANG Zhong, ZHOU Rui-xiang, WANG Zhuo-jian, JIA Wen-tong. Landing gear retraction system of modular modeling and thermal-hydraulic simulation [J]. Modular Machine Tool & Automatic Manufacturing Technique, 2013(3): 36−38. (in Chinese)

[5] LI Cheng-gong, JIAO Zong-xia. Calculation method for thermal-hydraulic system simulation [J]. Journal of Heat Transfer, 2008, 130(8): 084503.

[6] HAN Meng-hu, CAO Ke-qiang, HU Liang-mou, LI Yong-lin. Thermal model and simulation on hydraulic piston pump based on AMESim [J]. Machine Tool & Hydraulic, 2012, 40(1): 136−138. (in Chinese)

[7] WANG Jin-peng, QIN Si-cheng, ZHAO Ke-li. Thermal balance of hydraulic system of a 50 type wheel loader [J]. Journal of Jilin University (Engineering and Technology Edition), 2009, 39(3): 652−656. (in Chinese)

[8] LIANG Liang, TIAN Liang, QIN Gang, ZHANF Jie. Thermodynamic model and experimental study of twin tube hydraulic damper [J]. J Huazhong Univ of Sci & Tech (Natural

Science Edition), 2012, 40(8): 7−11. (in Chinese)
[9] YAO Jian-jun, FU Wei, HU Sheng-hai, HAN Jun-wei. Amplitude phase control for electro-hydraulic servo system based on normalized least-mean-square adaptive filtering algorithm [J]. Journal of Central South University of Technology, 2011, 18: 755−759.
[10] SAMANTARAY A K, BOUAMAMA B O. Model-based process supervision—A bond graph approach [M]. London: Springer Verlag, 2008: 22−43.
[11] KARNOPP D C, MARGOLIS D L, ROSENBERG R C. System dynamics: Modeling, simulation, and control of mechatronic systems [M]. New York: John Wiley & Sons, 2012: 548−590.
[12] MANDAL M, PAL S K. Pseudo-bond graph modeling of temperature distribution in a through-process steel rolling [J]. Mathematics and Computers in Simulation, 2008, 77(1): 81−95.
[13] ABBÈS M, FARHAT A, MAMI A, DAUPHIN-TANGUY G. Pseudo bond graph model of coupled heat and mass transfers in a plastic tunnel greenhouse [J]. Simulation Modelling Practice and Theory, 2010, 18(9): 1327−1341.
[14] LI Yong-lin, CAO Ke-qiang, XU Hao-jun, SU Xin-bing. Thermal-hydraulic modeling and simulation of hydraulic system based on Dymola [J]. Journal of System Simulation, 2010, 2(9): 2043−2047. (in Chinese)
[15] BOUAMAMA B O. Bond graph approach as analysis tool in thermofluid model library conception [J]. Journal of the Franklin Institute, 2003, 340(1): 1−23.
[16] IMAGINE S A. Thermal-Hydraulic Library User Manual [M]. 2010: 1−65.
[17] BORUTZKY W. Bond graph methodology: Development and analysis of multidisciplinary dynamic system models [M]. London: Springer Verlag, 2009: 438−455.
[18] MEDJAHER K, SAMANTARAY A K, OULD BOUAMAMA B. Bond graph model of a vertical U-tube steam condenser coupled with a heat exchanger [J]. Simulation Modelling Practice and Theory, 2009, 17(1): 228−239.
[19] WATTON J. Fundamentals of fluid power control [M]. New York: Cambridge University Press, 2009: 61−109.
[20] Van WYLEN G P, SONNTAG R E. Fundamentals of Classical Thermodynamics [M]. New York: Wiley, 2008: 90−160.
[21] KAZNESSIS Y N. Statistical thermodynamics and stochastic kinetics : An introduction for engineers [M]. New York: Cambridge University Press, 2011 : 1−79.

(Edited by YANG Bing)